TOXICOLOGICAL SCIENCES **125(2)**, 368–381 (2012)
doi:10.1093/toxsci/kfr309
Advance Access publication November 14, 2011

Lentiviral-Mediated RNAi Knockdown Yields a Novel Mouse Model for Studying Cyp2b Function

Basma Damiri,* Eric Holle,† Xianzhong Yu,†,‡ and William S. Baldwin*,‡,[1]

*Environmental Toxicology Program, Clemson University, Clemson, South Carolina 29634; †Clemson University Transgenic Facility, Greenville, South Carolina 29605; and ‡Department of Biological Sciences, Clemson University, Clemson, South Carolina 29634

[1]To whom correspondence should be addressed at Department of Biological Sciences, Clemson University, 132 Long Hall, Clemson, SC 29634. Fax: (864) 656-0439. E-mail: Baldwin@clemson.edu.

Received July 8, 2011; accepted November 8, 2011

There are few *in vivo* knockout models available to study the function of Cyp2 members involved in the metabolism of endogenous and exogenous chemicals. These models may help provide insight into the cytochrome P450s (CYPs) responsible for the detoxification and activation of drugs, environmental toxicants, and endobiotics. The aim of this work is to produce a potent Cyp2b-knockdown (KD) mouse for subsequent study of Cyp2b function. We made a quintuple Cyp2b-KD mouse using lentiviral-promoted short hairpin RNA (shRNA) homologous to all five murine Cyp2b subfamily members (Cyp2b9, 2b10, 2b13, 2b19, and 2b23). The Cyp2b-KD mice are viable, fertile, and without obvious gross abnormalities except for an increase in liver weight. Expression of the three hepatic Cyp2b members, 2b9, 2b10, and 2b13, is significantly repressed as demonstrated by quantitative real-time PCR and Western blotting. The constitutive androstane receptor activator, 1,4-Bis[2-(3,5-dichloropyridyloxy)] benzene (TCPOBOP), was used to determine if shRNA-mediated Cyp2b10 repression could be outcompeted by Cyp2b10 induction. TCPOBOP-treated Cyp2b-KD mice show 80–90% less Cyp2b protein expression than TCPOBOP-treated wild-type (WT) mice, demonstrating that Cyp induction does not outcompete the repressive function of the shRNA. Untreated and TCPOBOP-treated Cyp2b-KD mice are poor metabolizers of parathion compared with WT mice. Furthermore, Cyp2b-KD mice are sensitive to parathion, an organophosphate insecticide primarily metabolized by Cyp2b enzymes, when compared with WT mice. In summary, we designed an shRNA construct that repressed the expression and activity of multiple Cyp2b enzymes. We foresee that this novel Cyp2b-KD mouse model will significantly improve our understanding of the role of Cyp2b enzymes in chemical sensitivity and drug metabolism.

Key Words: **cytochrome; P450; Cyp2b; transgenics; organophosphates; metabolism.**

The cytochrome P450s (CYPs) are important in lipid metabolism, including the metabolism of fatty acids, retinoids, eicosanoids, steroids, vitamin D, bilirubin, bile acids, and xenobiotics. The CYPs in families 1–4 are important in the metabolism of xenobiotic chemicals with most of the drug metabolism being performed by CYP families 1–3 (Baldwin *et al.*, 2009; Hernandez *et al.*, 2009a; Muerhoff *et al.*, 1994; Waxman, 1988; Waxman *et al.*, 1991; Willingham and Keil, 2004). The CYP2 family contains several crucial subfamilies involved in detoxification, such as CYP2A, 2B, 2C, 2D, and 2E.

CYP2Bs participate in the metabolism of numerous xenobiotics, including parathion, malathion, diazinon, bupropion, efavirenz, and cyclophosphamide (reviewed in Hodgson and Rose, 2007; Wang and Tompkins, 2008). In some cases, CYP2B metabolism leads to chemical activation (Foxenberg *et al.*, 2007; Mutch and Williams, 2006; Tang *et al.*, 2001). The importance of CYP2B proteins as effective monooxygenases for environmental chemicals is illustrated by the fact that phenotyped human microsomes show a correlation between CYP2B6 content and increased production of metabolites of known CYP2B substrates (Hodgson and Rose, 2007). It is estimated that up to 12% of the available drugs on the market are metabolized by CYP2B6 (Wang and Tompkins, 2008), although CYP2B6 only makes up about 3–5% of the CYPs in the human liver (Lang *et al.*, 2004). However, CYP2B6 content varies as much as 100-fold between individuals (Ekins *et al.*, 1998), is sexually dimorphic (Lamba *et al.*, 2003) and polymorphic (Lang *et al.*, 2004), and these variances probably cause individual differences in the metabolism of these drugs.

Humans have one CYP2B gene, CYP2B6, whereas mice have five Cyp2b genes, Cyp2b9, Cyp2b10, Cyp2b13, Cyp2b19, and Cyp2b23 (Nelson *et al.*, 2004). Cyp2b9, Cyp2b10, and Cyp2b13 are the forms primarily expressed in the liver (Finger *et al.*, 2011). CYP2B6 in humans and Cyp2b10 in mice are transcriptionally regulated by the constitutive androstane receptor (CAR), a metabolic and xenobiotic sensing nuclear receptor (Honkakoski *et al.*, 1998; Kretschmer and Baldwin, 2005; Wang *et al.*, 2003; Zhang *et al.*, 2002). Perturbations in CAR activity are known to alter the metabolism and toxicity of bile acids (Beilke *et al.*, 2009; Uppal *et al.*, 2005), acetaminophen (Zhang *et al.*, 2002), and

parathion (Mota *et al*., 2010). However, Cyp2b's role in protecting individuals from these endogenous and exogenous chemicals is not fully understood as other detoxification enzymes are also regulated by CAR. Overall, the role of Cyp2b isoforms in mice and CYP2B6 in humans for metabolizing endogenous and exogenous chemicals is often overlooked and poorly understood in part due to the lack of an *in vivo* model (Reschly and Krasowski, 2006; Wang and Tompkins, 2008; Yamada *et al*., 2006).

Although there are *in vitro* models for studying many drug metabolizing CYPs, including recombinant Cyp2b isoforms, there are few *in vivo* models of CYP function, such as CYP-knockout mice. In fact, few of the detoxifying P450s with multiple isoforms have been knocked out. If not for the recent production of the Cyp3a-null (van Herwaarden *et al*., 2007) and Cyp2d-null mice (unpublished; available through Taconic) produced via cre-mediated deletion in the Cyp3a and Cyp2d clusters, there would be no CYP-null mice for P450 subfamilies with multiple isoforms. There are no CYP-null mice for any of the Cyp2 subfamily members critical in detoxification (i.e., Cyp2a, Cyp2b, Cyp2c, and Cyp2d) with the exception of Cyp2e1 (Lee *et al*., 1996), a one-member subfamily. There is also a Cyp2j5-null mouse (Athirakul *et al*., 2008); however, this CYP does not appear to have a significant role in detoxification.

Of the 68 functional CYPs in families 1–4, only 21 have been deleted. The primary reason that Cyp-null mice have rarely been made is because most murine Cyps in subfamilies 2–4 have many individual isoforms that may perform redundant functions. For example, the Cyp2b subfamily in mice has five isoforms (Nelson *et al*., 2004). Therefore, knocking out Cyp2b10 may have little effect on the physiology of the mouse because Cyp2b9, Cyp2b13, Cyp2b19, and Cyp2b23 with similar structures and potentially redundant functions are still available. In addition, the cost of making a quintuple knockout has made such inquiries impractical. Unlike the Cyp3a and Cyp2d clusters, the five Cyp2b genes are not found in a tandem repeat. Instead, the *Cyp2b9*/*10*/*13* repeat region is separated from the *Cy2b19*/*Cyp2b23* repeat region by five genes. Knocking out all five Cyp2b genes using a cre-recombinase system would also knockout five nontarget genes (Supplementary file 1).

Small interfering RNAs (siRNAs) are short double-stranded RNA molecules (21–25 nucleotides) that can form complementary sequences with single-stranded messenger RNAs (mRNAs), and in turn target them for degradation in a process called RNA interference (RNAi) (Elbashir *et al*., 2001). This leads to a decrease, but not the absence, of the expression of the corresponding protein. RNAi-mediated gene knockdown has been performed through several techniques at multiple levels, and the most successful application of RNAi has been to study gene function in cultured human and mouse cells. The generation of transgenic and knockout mouse models has been constantly improved, providing researchers with a large number of invaluable animal models. However, RNAi has not been used to knockdown whole subfamilies of Cyps, or produce efficient, persistent knockdown mice under the control of a lentiviral promoter that demonstrate the repression of multiple Cyps. Because the murine Cyp2b subfamily members show high homology, the Cyp2b subfamily can be targeted for short hairpin RNA (shRNA)–mediated repression. Therefore, we can potentially knockdown all five isoforms with one siRNA construct.

We used siRNA designed to repress the expression of each member of the murine Cyp2b subfamily. We hypothesized that the Cyp2b subfamily can be efficaciously knocked down in mice using lentiviral-driven shRNA homologous to each of the five Cyp2b subfamily members and the repression of the hepatic Cyp2b members; Cyp2b9/10/13 was tested in the liver of Cyp2b-knockdown (Cyp2b-KD) mice. Furthermore, we tested whether the repression of Cyp2b function caused changes in toxicant metabolism using the pesticide parathion. We envision that the Cyp2b-KD model will provide a new tool for further study of the impact of murine Cyp2b enzymes on the *in vivo* metabolism of endobiotic and xenobiotic chemicals.

MATERIALS AND METHODS

Design of Cyp2b constructs and generation of shRNA-containing lentiviruses. The five Cyp2b subfamily members were aligned with ClustalW (Fig. 1), and shRNAs were designed based on siRNA scales (http://gesteland.genetics.utah.edu/siRNA_scales) (Mateeva *et al*., 2007). Constructs of 21–22 base pairs (bp) were designed because previous work shows that dsRNA smaller than 23 bp do not elicit an antiviral interferon response that causes the cessation of all protein synthesis rather than elicit specific repression of a gene (Elbashir *et al*., 2001). Three different siRNA constructs (Cyp2b-KD2, Cyp2b-KD3, and scrambled) were chemically synthesized and cloned into the pRNAT-U6.2/Lenti plasmid at their BamH1 and Xho1 sites (Supplementary file 2). This plasmid also contains coral green fluorescent protein (cGFP) (Genscript, Piscataway, NJ) as a marker for expression.

Lentiviral particles were produced according to the manufacturer's instructions (Invitrogen, Carlsbad, CA). Human embryo kidney (293FT) cells (Invitrogen) were cultured in complete DMEM media containing 10% fetal bovine serum, 6mM L-glutamine, 1mM Modified Eagle's Medium (MEM) sodium pyruvate, 0.1mM MEM nonessential amino acids, and 500 μg/ml Geneticin (G418). One day before transfection, 5×10^6 cells were seeded in 10-cm dishes without G418. Twenty-four hours later, the cells were transfected with the pRNAT-U6.2/lenti plasmid from Genscript along with Virapower plasmids and Lipofectamine 2000 (Invitrogen) following the manufacturer's instructions. The next day, media-containing Lipofectamine was replaced with complete DMEM media, and 48 h later, the viral supernatant was collected, centrifuged, filtered through 0.45-μm low protein filter, and concentrated by ultracentrifugation (Burns *et al*., 1993; Ramezani and Hawley, 2002). The viral pellets were suspended in complete DMEM media with no antibiotic for perivitelline microinjection. Concentrated and unconcentrated viral stocks were titered and stored at −150°C.

Viral concentrations were determined according to the manufacturer's instructions (Invitrogen). HT1080 cells (Invitrogen) seeded in a six-well plate at 200,000 cells per well in complete DMEM media and 1% penicillin/streptomycin, were transduced with a serial dilution of the viral stocks, 6 μg/μl polybrene (Invitrogen), and incubated at 37°C overnight in a humidified 5% CO_2 incubator. The following day, the media were changed to complete DMEM media and G418 (350 μg/ml) to select the transduced cells. Media were

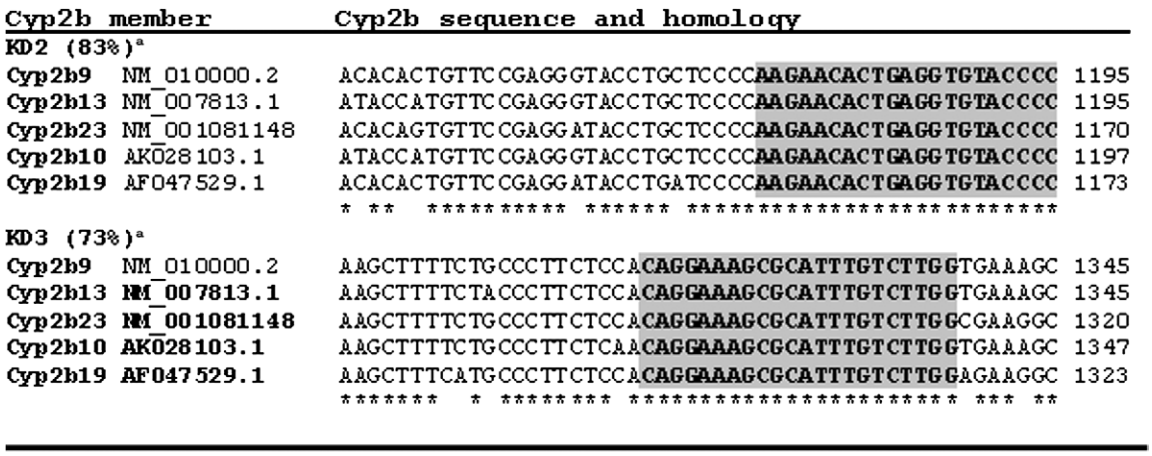

FIG. 1. siRNA target areas for mouse Cyp2b genes. There are five areas of the mouse Cyp2b subfamily that are sufficiently conserved so that all the Cyp2bs could potentially be knocked down by the same siRNA. siRNA scales estimate a greater than 70% knockdown (shown in parenthesis[a]) of Cyp2b expression using two of these siRNAs (shown in gray). shRNA constructs were made to KD2 and KD3 and inserted into the pRNAT-U6.2/lenti vector. NCBI accession numbers are provided next to the name of each Cyp2b gene. Numbers on the right indicate sequence length near the area of homology.

replaced every 3–4 days with fresh media containing G418. Titer was determined by counting the percentage of positive cells (green cells) with an inverted fluorescent microscope after 5–7 days of transduction, or colonies were counted after 2 weeks of G418 exposure (Blesch, 2004; Sastry *et al*., 2002). Lentiviral titers were 1.0, 1.2, and1.5×10^6 transduction units (TU) per ml for Cyp2b-KD2, Cyp2b-KD3, and scrambled, respectively. Concentrated lentiviral titers for Cyp2b-KD2, Cyp2b-KD3, and the scrambled construct were 3×10^8, 5×10^8, and 1×10^8 TU, respectively.

Primary hepatocyte transduction. Primary mouse hepatocytes (CellzDirect, Pittsboro, NC) from male CD-1 mice plated in 12-well plates (128,000 cell per well) were transduced with either Cyp2b-KD2, Cyp2b-KD3, or scrambled constructs at a multiplicity of infection (MOI) of 5 or 20. Twenty-four hours after transduction, the cells were treated with the CAR activator 1,4-Bis[2-(3,5-dichloropyridyloxy)] benzene (TCPOBOP) (Sigma Aldrich, St Louis, MO) to induce Cyp2b subfamily members (especially Cyp2b10). Cells were harvested for RNA extraction and quantitative real-time PCR (QRT-PCR) 24 h after TCPOBOP treatment. In addition, the percentage of cells infected based on the presence of green fluorescence using fluorescent microscopy (Zeiss Axiovert 200M; Carl Zeiss International, Gottingen, Germany) was determined so that the drop in Cyp2b expression could be compared with the number of cells transduced.

Perivitelline injections. Donor FVB/NJ (FVB; wild-type [WT]) female mice (The Jackson Laboratory, Bar Harbor, ME) were superovulated and mated to FVB stud males. Donor females showing vaginal plugs were sacrificed. The single-cell embryos were washed several times in micro drops of M16 medium (Millipore, Billerica, MA) and used in microinjection. Concentrated Cyp2b-KD2 lentivirus (8 plate per cell) suspended in DMEM media or PBS at concentrations of approximately 5×10^8 TU were injected into the perivitelline space of fertilized single-cell FVB embryos. The zygotes then were cultured overnight and transplanted into pseudopregnant CD-1 mice the next morning.

Genotyping. Viral and siRNA integration were detected by PCR analysis and confirmed by sequencing. Total genomic DNA was isolated from mice tail biopsies with the DNeasy blood and tissue DNA extraction kit following the manufacturer's instructions (Qiagen, Valencia, CA). Primers spanning the shRNA were used in PCR to genotype the mice. These primers, pRNAT-U.6/Lenti-specific primers and Cyp2b-KD, amplify 956 and 359 bp targets, respectively, within the promoter and shRNA and are available in Supplementary file 3. Genotyping results were determined from PCR reactions run on 1.6% agarose gels. To confirm the PCR results, the PCR product was purified using the MinElute PCR Purification Kit (Qiagen) and sequenced.

Mice treatments. All studies were carried out according to the National Institutes of Health guidelines for the humane use of research animals and preapproved by Clemson University's Institutional Animal Care and Use Committee. Mice were provided water and fed *ad libitum* prior to and during treatments. WT (FVB/NJ) mice from The Jackson Laboratory were bred to positive Cyp2b-KD2 mice to maintain the genetic background. Untreated WT and Cyp2b-KD2 mice were euthanized at 8–12 weeks of age ($n = 4$–8) to investigate differences in Cyp2b expression. In addition, 8- to 12-week-old WT and Cyp2b-KD mice were injected ip with 3 mg/kg TCPOBOP or vehicle (corn oil) to investigate Cyp2b expression following treatment with a CAR activator and Cyp2b inducer (Tzameli *et al*., 2000; Wei *et al*., 2000). Mice were weighed prior to treatment. Twenty-four hours after treatment, mice were euthanized, livers excised and weighed, and then cut into three pieces for sample preparation (RNA, protein, and histopathology).

Sample preparation. A portion of the liver was placed in 10% formalin (Fisher Scientific, Pittsburgh, PA) for histology investigations. The rest of the liver was snap frozen, diced, separated into two tubes, and placed in a freezer at −80°C for further preparation. Total RNA was extracted from one third of the liver using modified phenol/chloroform extraction technique with TRI-Reagent according to the manufacturer's instructions followed by DNase digestion to remove residual genomic DNA (Promega Corporation, Madison, WI). RNA concentrations were determined spectrophotometrically at 260/280 nm (Molecular Devices, Ramsey, MN). Reverse transcription was performed to make complementary DNA (cDNA) using 200 units Moloney murine leukemia virus-reverse transcriptase, a 10mM deoxynucleotide triphosphate mixture, and 0.05 mg random hexamers (Promega Corporation). RNA was stored at −80°C, and cDNA was stored at −20°C.

For cytosol and microsome preparation, the liver was individually homogenized with a dounce homogenizer, and protein fractions were prepared by differential centrifugation (Van der Hoeven and Coon, 1974). Protein concentrations were determined from cytosol and microsomes using the Bio-Rad protein assay according to the manufacturer's instructions (Bio-Rad Laboratories, Hercules, CA). Microsomes and cytosol were stored at −80°C.

Quantitative real-time PCR. QRT-PCR was performed using primers for specific isoforms to Cyp2b9, Cyp2b10, and Cyp2b13 subfamily members and 18S or β-actin as the housekeeping genes (Supplementary file 3). For primary mouse hepatocytes, cDNA was diluted 1:5 prior to QRT-PCR. To generate a standard curve and determine the PCR efficiency of each reaction, a composite sample of cDNA from treated and untreated cells was made with dilutions of

1:1, 1:5, 1:50, and 1:500. For Cyp2b10, a TaqMan probe was used, and β-actin was the housekeeping gene; for Cyp2b9, SYBR Green qPCR Master Mix was used, and 18S ribosomal RNA was the housekeeping gene.

For studies with mice, Cyp2b9, Cyp2b10, Cyp2b13, and CAR were quantified from liver cDNA samples that were diluted 1:10 prior to QRT-PCR (Supplementary file 3). To generate a standard curve and determine the PCR efficiency of each reaction, a composite sample of cDNA from treated and untreated WT and Cyp2b-KD mice was made, and dilutions from 1:1 to $1:10^{-6}$ were prepared. Amplification of the samples and the standard curve was performed in triplicate using a 96-well iQ5 multicolor real-time PCR detection system (Bio-Rad) with 0.25× SYBR Green qPCR Master Mix (SABiosciences, Frederick, MD) as the fluorescent double strand-intercalating agent to quantify gene expression as described previously (Hernandez *et al*., 2006; Mota *et al*., 2010). Muller's equation was used to determine relative quantities of each CYP (Muller *et al*., 2002). A minimum of 40 cycles was run on all real-time samples to ensure a log-based growth curve.

Immunoprecipitations and Western blots. CAR was immunoprecipitated prior to quantification by Western blotting as described previously (Hernandez *et al*., 2009b). This CAR antibody (SC-13065; Santa Cruz Biotechnology, Santa Cruz, CA) has been demonstrated to specifically recognize CAR and does not recognize any nuclear proteins in CAR-null mice (Hernandez *et al*., 2007).

Western blots were also performed using 30–50 μg of hepatic microsomal protein to detect and quantify Cyp2b protein levels with a primary antibody developed in our laboratory that has increased sensitivity toward Cyp2b proteins (Mota *et al*., 2010, 2011). A peptide (LHDPQYFEQPDSFN-C-Keyhole-Limpet-Hemocyanin) that recognizes Cyp2b9, Cyp2b10, Cyp2b13, and Cyp2b19 was used to make and purify a rabbit anti-mouse polyclonal antibody (Mota *et al*., 2010). The peptide is poorly conserved between Cyp2b and other Cyp enzymes. Cyp2b10 is highly inducible by CAR activators and slightly larger (56.7 kDa compared with 55.7 kDa for Cyp2b9 and 55.8 kDa for Cyp2b13; www.uniprot.org) because it is nine amino acids larger than Cyp2b9 and Cyp2b13. Therefore, the higher band in females and following TCPOBOP treatment is most likely Cyp2b10, whereas the band expressed constitutively in females is predominantly Cyp2b9 with some Cyp2b13 as these Cyps are highly female predominant (Hashita *et al*., 2008; Hernandez *et al*., 2006; Jarukamjorn *et al*., 2006).

β-actin (Sigma Aldrich) was used as a housekeeper to ensure equal loading of samples (Mota *et al*., 2010). Goat anti-rabbit IgG (Bio-Rad) alkaline phosphatase–coupled secondary antibodies were used for recognizing the Cyp2b primary antibody, and goat anti-mouse (Bio-Rad) IgG was used to recognize β-actin primary antibodies. All bands were visualized with chemiluminescence detection using the Immun-Star AP Chemiluminescent Protein Detection System and quantified with the Chemi Doc XRS HQ using Quantity One 4.6.5 software (Bio-Rad Laboratories).

Parathion metabolism. Changes in parathion metabolism were examined with 250 μg of liver microsomes from untreated and TCPOBOP-treated WT and Cyp2b-KD2 mice (Foxenberg *et al*., 2007; Mota *et al*., 2010; Mutch *et al*., 1999). Samples were incubated in buffer (0.1M Tris-HCl and 5mM $MgCl_2$ at pH 7.4) and 20μM parathion at 37°C in the presence of the esterase inhibitors 1mM EDTA and 50μM iso-OMPA. Reactions were initiated with 1mM NADPH and stopped after 60 min with 500 μl of methanol/0.1% phosphoric acid. The assay rates are linear in WT mouse microsomes for 30 min; however, nondetection is common in transgenic mice with low Cyp2b expression (Mota *et al*., 2010). Therefore, the assays were extended to 60 min, a time point that continues to show increasingly greater metabolite concentrations even in WT mouse microsomes. Metabolite concentrations from filtered (0.22 μm, PTFE filter; Fisher Scientific) samples were measured by reverse phase high performance liquid chromatography (HPLC) as described previously (Mota *et al*., 2010). Chemical detection was determined at 275 nm for parathion and paraoxon (POXON) and at 310 nm for *para*-nitrophenol (PNP). The detection limit for POXON is 0.0275 μg/ml, and the detection limit for PNP is 0.0139 μg/ml.

Histopathology. To evaluate the histopathological effect of Cyp2b repression on Cyp2b-KD mice, liver samples from male and female, corn oil and TCPOBOP-treated, WT, and Cyp2b-KD mice ($n = 3$) were fixed in 10% formalin. Samples were processed and stained with hematoxylin and eosin at Colorado Histo-Prep for blind histopathological evaluation (Fort Collins, CO). Standardized toxicological pathology criteria and nomenclature for the mouse were used to categorize microscopic tissue changes (Banks, 1993; Percy and Barthold, 2001). Parameters examined were hepatocellular swelling, necrosis, hypertrophy, hyperplasia, inflammation, bile duct hyperplasia, and mineralization. The individual parameters were scored 0–4 and then summed. There is considered minimal pathology if the mouse liver scored less than 5, mild pathology if the total score is 5–10, moderate pathology if the total score is 10–15, and marked pathology if the total score is 15–20. Total scores for the hepatic histopathology lesions in each mouse were ranked, and statistical significance determined by two-way ANOVA followed by Bonferroni posttest using GraphPad Prism 4.0 (GraphPad Software, San Diego, CA).

Zoxazolamine. Untreated male and female mice from WT and Cyp2b-KD mice ($n = 5$–15) were injected ip with 400 mg/kg zoxazolamine (Zox). Paralysis time was measured by placing paralyzed mice on their backs and measuring the time until they were able to right themselves consistently (Hernandez *et al*., 2007). Mice that did not recover from Zox-induced paralysis within 8 h were euthanized.

Parathion toxicity. Both male and female, WT, and Cyp2b-KD mice ($n = 5$–15 per treatment) were injected ip in the morning with 5 mg/kg/day of parathion, and behavioral changes observed over the next 6 h as described previously (Mota *et al*., 2010). The severity of toxicity was quantified based on these symptoms: 0 = not toxic, 1 = eye leakage, 2 = slow tremors, 3 = morbid, and 4 = death. Mice showing severe toxicity were immediately euthanized.

Statistical analysis. Results are expressed as mean ± SEM. Tests of significance (GraphPad Prism 4.0) were conducted by unpaired Student's *t*-test or ANOVA followed by Tukey's *post hoc* test when multiple treatments were compared. A p value < 0.05 is regarded as statistically significant. Differences in the number of mice paralyzed by Zox were determined by the Mann-Whitney rank sum test. Parathion toxicity was determined statistically with behavioral rankings as described previously (Mota *et al*., 2010) using the Kruskal-Wallis nonparametric test for independent variables followed by Dunn's *post hoc* test.

RESULTS

Design and Determine the Efficacy of the Cyp2b shRNA Constructs

ClustalW alignments of the five Cyp2b subfamily members demonstrated that there are five highly homologous areas of the murine Cyp2bs. shRNA constructs that recognize all five Cyp2b subfamily members in mice were designed based on these homologous areas. Two of these sites, designated KD2 and KD3, respectively (Fig. 1), are potential targets for shRNA based on siRNA scales (Mateeva *et al*., 2007) that indicates these constructs would repress Cyp2b expression greater than 70% in cell culture.

In addition, each construct was compared with several other CYP genes to make sure that they were not homologous to other CYPs and cause the repression of their expression. The homologous region of Cyp2a4 is 57% identical to the Cyp2b-KD2 construct; all other Cyps examined showed less than 50% identity to the Cyp2b-KD2 shRNA construct. Homologous regions of Cyp2c29 and Cyp2c37 showed 82 and 73% identity to the Cyp2b-KD3 construct (Supplementary

TABLE 1
Relative Cyp2b Expression in Primary Hepatocytes Transduced with Cyp2b-KD2 and -KD3 shRNA Compared with Hepatocytes Transduced with a Scrambled Construct

CYP	Scrambled	KD2 (5 MOI)	KD2 (20 MOI)	KD3 (20 MOI)
Cyp2b9	1.0	0.11	0.02	1.41
Cyp2b10	1.0	0.27	0.30	0.36

file 4). All other Cyps examined showed less than 60% identity to the Cyp2b-KD3 shRNA constructs.

The efficacy of Cyp2b-KD2 and -KD3 lentiviral shRNA constructs to repress Cyp2b9 and Cyp2b10 expression was tested using primary mouse hepatocytes. The percentage of cells infected based on the presence of green fluorescence using fluorescent microscopy was approximately 80% in KD2-transduced cells at an MOI of 5 and about 70% in KD3-transduced cells at an MOI of 5. Cyp2b-KD2 reduced Cyp2b9 and Cyp2b10 expression 73–98% (Table 1). This suggests that the cells that were infected showed nearly a complete abolishment of these Cyp2b subfamily members. Cyp2b-KD3 was not as efficacious. It reduced Cyp2b10 expression 50% following infection of 70% of the cells; however, KD3 did not repress Cyp2b9 expression relative to cells treated with the scrambled shRNA (Table 1). Because Cyp2b-KD2 is more efficacious, and Cyp2b-KD3 does not reduce Cyp2b9 expression and shows higher homology to other Cyp2 members, transgenic mice were made with the Cyp2b-KD2 construct.

Generation of RNAi Transgenic Mice

Engineered lentiviral Cyp2b-KD2 particles were micro-injected into the perivitelline space of FVB/NJ mouse zygotes. Perivitelline injection of FVBs produced 134 pups, of which 100% were positive, by PCR genotyping of the tail clippings (Supplementary file 5). DNA sequencing confirmed the existence of the Cyp2b-KD2 construct in our mice. In addition, newborn mice were screened for GFP under an ultraviolet light, and only three mice visually expressed GFP 7 days after birth. Several of these mice continued to show fluorescence in the ears, tail, feet, and especially the eyes when adults. None of the F1 or F2 generation mice tested showed brilliant green skin expression, but some of them expressed green teeth. Five transgenic founders (four males and one female) identified based on genotyping and sequencing results were mated to FVB/NJ mice to obtain F1 progeny. All F0 mice were able to give rise to transgenic offspring. Nearly 86% of the F1 mice are positive after mating positive F1 to FVB/NJ mice. The high percentage of positive F1 mice indicates that our F0 Cyp2b-KD mice had multiple integrants. All the transgenic mice have developed and bred normally. In addition, none of the mice show obvious spontaneous abnormalities except for a significant increase in liver/body weight ratios (hepatosomatic index) compared with WT mice. The hepatosomatic index increased 21–22% ($p < 0.0001$) in males and females, respectively.

Efficacy of Cyp2b Repression in Cyp2b-KD Mice

QRT-PCR and Western blots were performed to measure changes in the expression of individual Cyp2b isoforms in WT and Cyp2b-KD mice. Cyp2b9, Cyp2b10, and Cyp2b13 are female predominant Cyps (Hashita *et al*., 2008; Jarukamjorn *et al*., 2006) in FVB mice (Hernandez *et al*., 2006), although there is some disagreement as to whether Cyp2b10 is female predominant (Jarukamjorn *et al*., 1999), and this may be caused by strain differences (Hernandez *et al*., 2009b). QRT-PCR of untreated adult WT and Cyp2b-KD mice indicate that most but not all the hepatic Cyp2b members are repressed in the KD mice. The expression of Cyp2b9, Cyp2b10, and Cyp2b13 are repressed in male Cyp2b-KD mice relative to WT mice. In contrast, only Cyp2b10 and Cyp2b13 are repressed in female Cyp2b-KD mice relative to their WT controls (Fig. 2). Cyp2b9, a female predominant Cyp that is expressed at greater levels than the other Cyp2b members constitutively (Lee *et al*., 2011; Sutton *et al*., 2010), is not repressed in females.

Western blots demonstrate that Cyp2b protein expression is also repressed. Two distinct Cyp2b members, thought to be Cyp2b9 and Cyp2b10, are repressed in females (Fig. 2), indicating that Cyp2b protein expression is reduced in the female Cyp2b-KD mice. Untreated male mice have low Cyp2b expression (Hernandez *et al*., 2006, 2009b), and our antibody was not sensitive enough to consistently quantify Cyp2b levels in the WT or Cyp2b-KD mice. Therefore, we also measured Cyp2b expression in TCPOBOP-treated mice.

The CAR activator, TCPOBOP (Tzameli *et al*., 2000), was used to determine the efficacy of our Cyp2b-KD construct at reducing Cyp2b levels following treatment with a powerful inducer. The primary purpose of this experiment was to determine if TCPOBOP treatment and the subsequent Cyp2b induction would outcompete lentiviral-promoted shRNA repression of Cyp2b. None of the hepatic Cyp2bs showed lower transcript expression after TCPOBOP treatment in the Cyp2b-KD mice compared with the WT mice (Fig. 3). Cyp2b10 and Cyp2b13 showed greater expression in the TCPOBOP-treated Cyp2b-KD female mice than the WT mice by 2.6×, indicating a compensatory mechanism. However, protein levels as determined by Western blots did not confirm the QRT-PCR results and actually showed significant decreases in Cyp2b expression (about 5–10×) in the Cyp2b-KD mice compared with the WT mice (Fig. 3). This demonstrates that TCPOBOP-mediated Cyp2b induction did not outcompete the shRNA's ability to repress Cyp2b protein expression. Therefore, the Cyp2b-KD mouse was still functionally repressing Cyp2b protein concentrations even after the addition of a potent Cyp2b inducer.

CAR constitutively regulates the expression of Cyp2b10 and Cyp2b13 (Hernandez *et al*., 2009b; Mota *et al*., 2010) and may

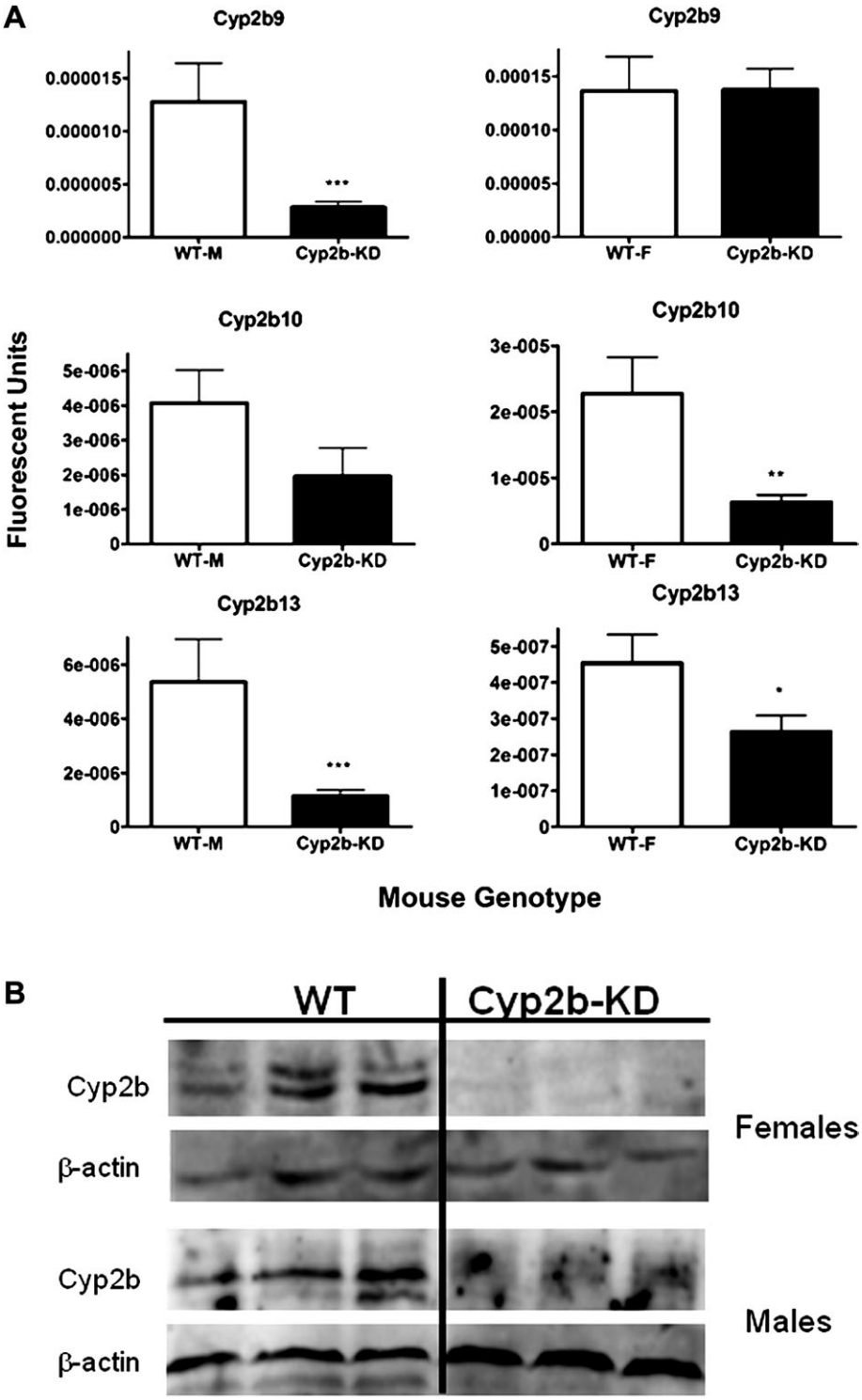

FIG. 2. Hepatic Cyp2b expression in WT and Cyp2b-KD mice as demonstrated by QRT-PCR (A) and Western blots (B). Data were expressed as mean ± SEM (n = 5–8). Statistical significance was determined by Student's t-test using the GraphPad Prism 4.0 software package. Significant differences at $^{*}p < 0.05$, $^{**}p < 0.01$, and $^{***}p < 0.001$. WT = wild-type, KD = Cyp2b-KD mice, M = male, and F = female. Expression was not quantified in the Western blots because of the low expression of Cyp2bs in the male mice and Cyp2b-KD female mice.

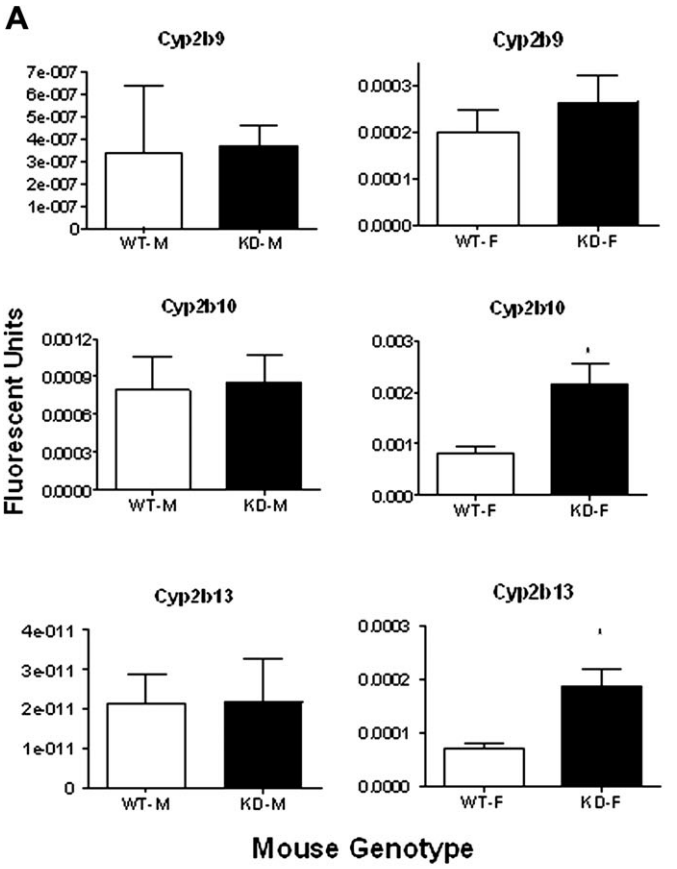

FIG. 3. Hepatic Cyp2b expression in WT and Cyp2b-KD mice treated with the Cyp2b10 inducer, TCPOBOP. (A) RNA expression of Cyp2b9, Cyp2b10, and Cyp2b13 as measured by QRT-PCR (n = 5–8). (B) Protein expression of hepatic Cyp2b subfamily members (n = 3–4). Data were expressed as mean ± SEM. Statistical significance was determined by Student's t-test using the GraphPad Prism 4.0 software package. *$p < 0.05$ and **$p < 0.01$. WT = wild-type, KD = Cyp2b-KD mice, M = male, and F = female.

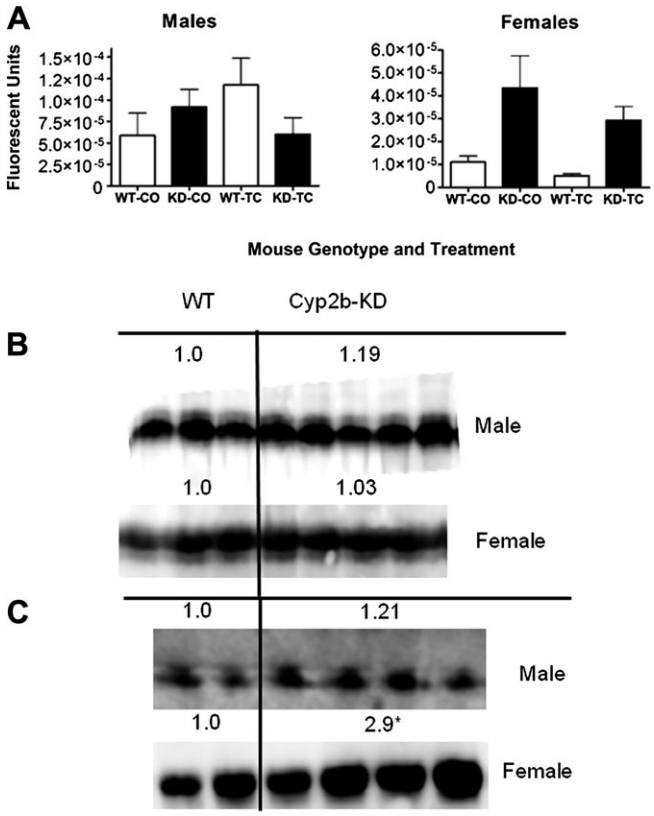

FIG. 4. Hepatic expression of CAR in WT and Cyp2b-KD mice treated with TCPOBOP or corn oil (carrier) as measured by QRT-PCR (A) or Western blots (B, C). (A) WT mice are shown in white bars, and Cyp2b-KD mice are shown in black bars. Statistical significance was determined by ANOVA followed by Dunnett's *post hoc* test with the GraphPad Prism 4.0 software package. Western blots in corn oil (B) or TCPOBOP-treated mice (C). Statistical significance of the Western blots was determined by Student's t-test. An asterisk indicates significant difference with a $p < 0.05$.

constitutively regulate the expression of Cyp2b9 in males (Mota *et al.*, 2010). Therefore, we hypothesized that CAR transcript expression may be increased in the Cyp2b-KD mice as a compensatory mechanism that increases CAR's sensitivity to endogenous ligands or its constitutive activity and in turn increases Cyp2b expression, especially Cyp2b10. QRT-PCR and Western blotting were performed (Fig. 4), and QRT-PCR suggested that CAR may be increased in female Cyp2b-KD mice relative to WT mice, but the data were not statistically significant ($p = 0.061$). Western blots were performed to confirm QRT-PCR results and ascertain whether there was a trend suggesting increased CAR in females. CAR protein expression was significantly increased (2.9×) in the TCPOBOP-treated Cyp2b-KD female mice but not the untreated mice compared with the corresponding WT mice, suggesting that CAR may be involved in a compensatory mechanism that helps Cyp2b-KD mice respond to a chemical insult, such as TCPOBOP (Fig. 4); however, the compensatory mechanism did not overcome the ability of the shRNA construct to repress Cyp2b protein expression in the mice.

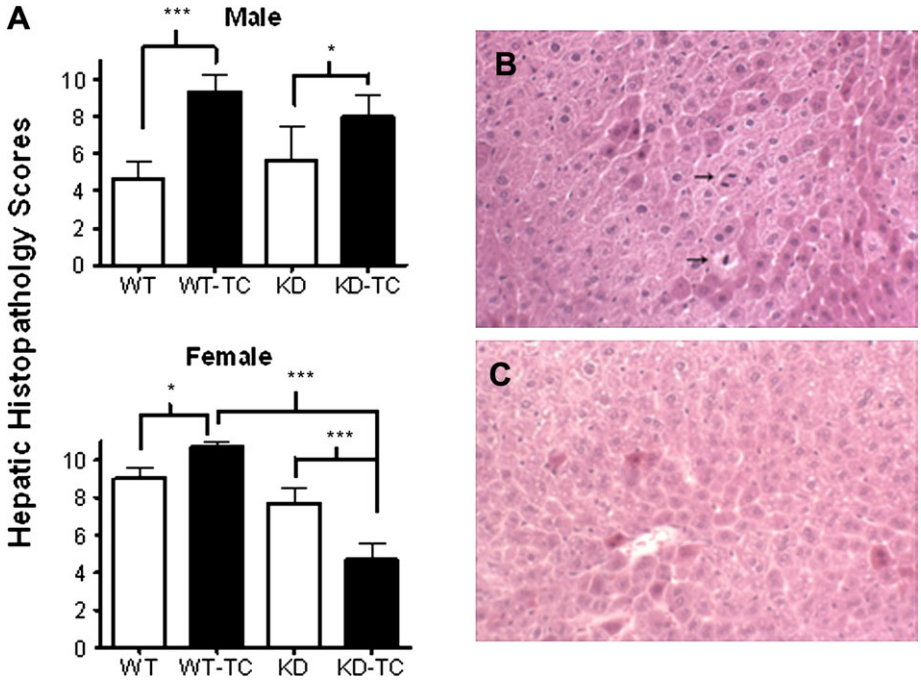

FIG. 5. Histopathology of WT and Cyp2b-KD (KD) mice treated with corn oil or TCPOBOP (TC). (A) Histopathology was measured as described in the ''Materials and Methods'' section using a combined histopathology score from several different measures. Asterisks indicate statistical differences (*$p < 0.05$; **$p < 0.01$; and ***$p < 0.001$) as determined by a two-way ANOVA followed by a Bonferroni posttest ($n = 3$). (B) Female WT mouse showing hyperplasia after TC treatment (200×). (C) Female Cyp2b-KD mouse showing no discernable hyperplasia after TC treatment (200×).

Histopathology

Because CAR is critical in hepatic responses to toxicants, we investigated whether Cyp2b-KD mice may show histopathological changes especially after TCPOBOP treatment. Summation of the different histopathology parameters examined indicates that only the TCPOBOP-treated Cyp2b-KD female mice responded in an atypical manner (Fig. 5). For example, all the TCPOBOP-treated male and female WT mice showed increased combined histopathology scores primarily because of increased hyperplasia, typical of TCPOBOP-treated mice (Blanco-Bose *et al.*, 2008; Wei *et al.*, 2000). However, TCPOBOP-treated Cyp2b-KD female mice had significantly decreased combined histopathology scores compared with TCPOBOP-treated WT mice and control (corn oil) Cyp2b-KD mice (Fig. 5). Only eight mice showed a score of 6 or less; this includes all three female TCPOBOP-treated Cyp2b-KD mice. The other mice with scores of less than 6 were all control mice (three male control WT and two control Cyp2b-KD mice). The two-way ANOVA indicates that low mineralization and hyperplasia are the primary reasons for low combined histopathology scores in the TCPOBOP-treated Cyp2b-KD female mice ($p < 0.05$). Hypertrophy is also decreased in the TCPOBOP-treated Cyp2b-KD mice but not significantly. There were no significant differences between the groups when examining swelling, inflammation, bile duct hyperplasia, or necrosis.

Cyp2b-Mediated Metabolism Is Compromised in the Cyp2b-KD Mice

The *in vitro* metabolism of parathion was examined in liver microsomes from untreated and TCPOBOP-treated mice to test whether Cyp2b-KD mice demonstrated perturbed metabolism of parathion relative to WT mice. Cyp2b enzymes have a high affinity for parathion and in turn are probably key enzymes in the metabolism of parathion to its toxic form paraoxon (POXON) and its nontoxic form PNP (Foxenberg *et al.*, 2007, 2011; Mota *et al.*, 2010). Parathion metabolism was severely compromised (down 3–7×) in the untreated male and female Cyp2b-KD mice compared with the untreated WT mice (Figs. 6A and 6B). Parathion metabolism was compromised even more in the TCPOBOP-treated Cyp2b-KD mice compared with the TCPOBOP-treated WT mice (down 5–8×) (Figs. 6C and 6D) consistent with the Western blot results demonstrating lower Cyp2b expression in TCPOBOP-treated CYP2b-KD mice than WT mice. Overall, PNP production was compromised 42.9% more than POXON production in the Cyp2b-KD mice, which means the ratio of PNP over POXON was higher in the WT mice than the Cyp2b-KD mice. A higher ratio indicates greater production of the nontoxic metabolite and may provide a protective effect. Untreated male and female WT mice had PNP/POXON ratios of 6.2 and 7.9, respectively; and TCPOBOP-treated WT mice had PNP/POXON ratios of 7.2 and 6.6, respectively. Untreated male

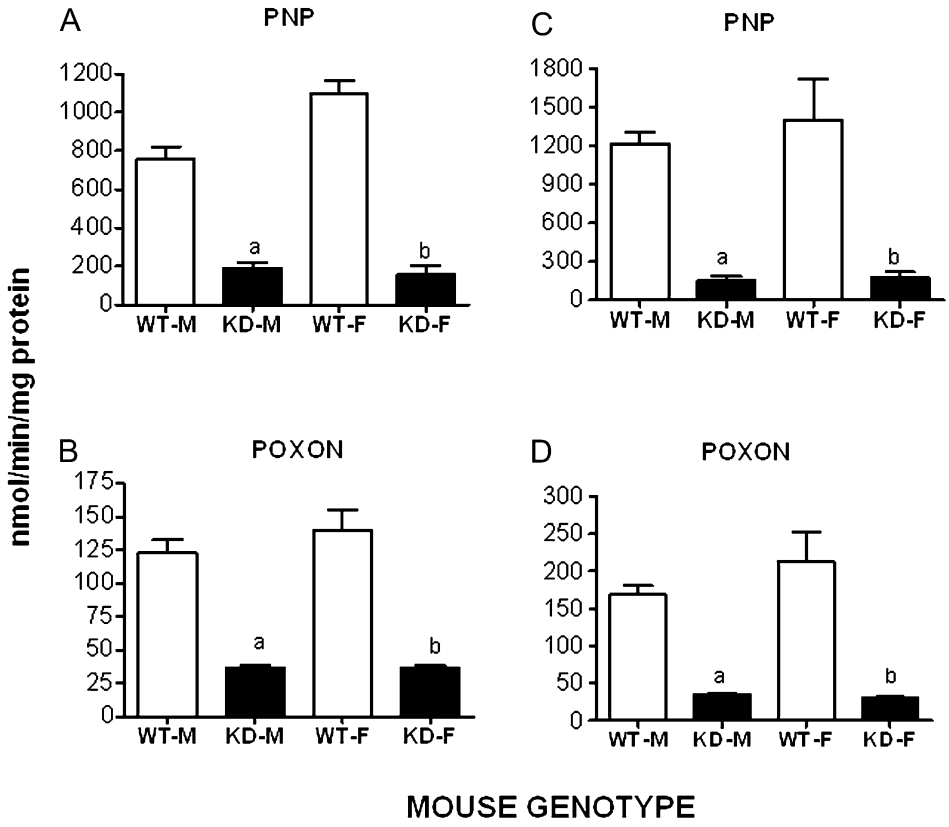

FIG. 6. Microsomal metabolism of parathion. Microsomes from control and TCPOBOP-pretreated WT and Cyp2b-KD mice were prepared and incubated with 20μM parathion for 60 min. The formation of parathion's relatively nontoxic metabolite, PNP, and its toxic metabolite paraoxon (POXON) was quantified by HPLC as described in the ''Materials and Methods'' section. (A) PNP and (B) POXON formation in microsomes from untreated WT and CYP2b-KD mice. (C) PNP and (D) POXON formation in microsomes from TC-pretreated WT and Cyp2b-KD mice. A white bar indicates WT mice, and a black bar indicates Cyp2b-KD mice. Significant differences in the formation of the metabolites between WT and Cyp2b-KD mice were assessed by ANOVA followed by Tukey's multiple comparison test using the GraphPad Prism 4.0 software package. The letter ''a'' indicates a significant difference between WT and Cyp2b-KD males ($p < 0.01$), and the letter ''b'' indicates a significant difference between WT and Cyp2b-KD females ($p < 0.01$).

and female Cyp2b-KD mice had PNP/POXON ratios of 5.1 and 4.2, respectively, and TCPOBOP-treated male and female Cyp2b-KD mice had PNP/POXON ratios of 4.4 and 5.8, respectively.

Toxicological Changes in Cyp2b-KD Mice

Zox is a classical CYP substrate used to estimate the functional *in vivo* effects of perturbations in CYP activity, as increased paralysis indicates inhibition or repression of CYPs and decreased paralysis indicates induction (Hernandez *et al.*, 2007; Wei *et al.*, 2000). Untreated Cyp2b-KD female mice were extremely sensitive to Zox treatment as 50% of Cyp2b-KD female mice died 4–5 h after Zox treatment, and the other 50% were euthanized as they had not recovered from ZOX-induced paralysis after 8 h (Table 2). In comparison, WT female mice showed little toxicity to Zox-induced paralysis. None of the WT female mice were paralyzed by 400 mg/kg Zox but three of the five WT females did show slow erratic movements for 10–15 min after injection. Males did not show a significant difference in Zox paralysis times as few of the WT or CYP2b-KD mice showed significant paralysis, although there appeared to be increased ''shaking'' that lasted hours in the Cyp2b-KD mice.

CAR-null mice showed reduced parathion metabolism and increased toxicity (Mota *et al.*, 2010). CAR-null mice also have reduced expression of several CYPs including several Cyp2b

TABLE 2
Zox-Induced Paralysis in Cyp2b-KD Mice Compared with WT Mice

Mouse strain	Male[a]	Female[a]
WT	1/7	0/5
Cyp2b-KD	1/7	15/15*

[a]Data are shown as number of mice showing paralysis/number of mice treated with 400 mg/kg Zox.

*Indicates a significant difference in the percentage of female mice paralyzed by Zox when compared with the corresponding WT mice Fisher's exact test (GraphPad Prism 4.0).

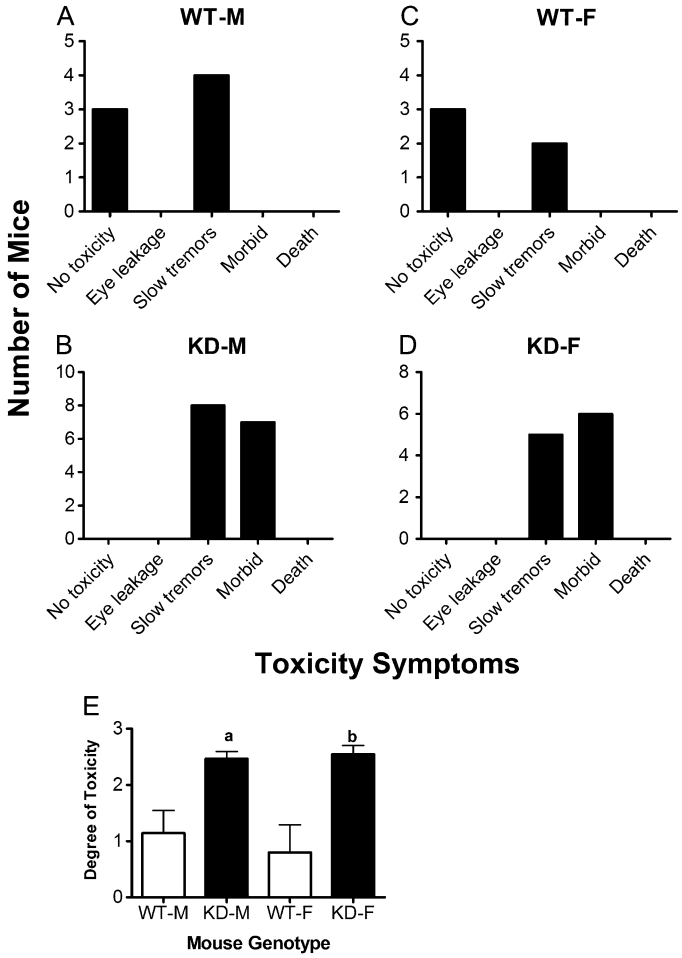

FIG. 7. Increased toxicity of parathion in Cyp2b-KD mice compared with WT mice. (A) WT male mice treated with parathion. (B) Cyp2b-KD male mice treated with parathion. (C) WT female mice treated with parathion. (D) Cyp2b-KD female mice treated with parathion. (E) Overall, differential toxicity to parathion in Cyp2b-KD mice compared with WT mice. A significant increase in toxicity to parathion was observed in Cyp2b-KD mice as determined by the Kruskal-Wallis nonparametric test for independent variables followed by Dunn's *post hoc* test using the GraphPad Prism 4.0 software package. Severity of toxicity: 0 = not toxic; 1 = eye leakage; 2 = lethargy/tremors; 3 = morbidity; and 4 = death ($p < 0.05$). WT = wild-type, KD = Cyp2b-KD mice, M = male, and F = female.

members (Hernandez *et al*., 2009b; Mota *et al*., 2010). Because we observed that Cyp2b-KD mice are also poor parathion metabolizers using *in vitro* assays, we examined toxicity induced by parathion *in vivo*. Both Cyp2b-KD males and females showed increased sensitivity to parathion at 5 mg/kg compared with WT mice (Fig. 7). Initial toxicity was shown by mucous discharge from the eyes and later reduced activity, lethargy, significant morbidity, or death. All the Cyp2b-KD mice showed toxicity symptoms, and some of the Cyp2b-KD mice showed morbidity. None of the WT mice showed morbidity, a few were lethargic, but almost 50% of the WT mice showed no overt toxicity to parathion. Moreover, WT mice recovered faster than the Cyp2b-KD mice, indicating that Cyp2bs are key enzymes in the detoxification of parathion, and a lack of metabolic activity toward parathion probably increases the retention of paraoxon and its subsequent toxicity.

DISCUSSION

The Cyp2b subfamily in mice has undergone significant gene duplication. In contrast, humans have only one CYP2B subfamily member. Reduced CYP subfamily members in humans compared with mice are common (Nelson *et al*., 2004). The redundancy of murine Cyp2bs in each subfamily makes individual targeted mouse gene knockouts impractical and costly because if one Cyp is eliminated, there are still four other Cyp2bs available to carry out potentially redundant functions. To circumvent this limitation, we designed and determined an efficient shRNA construct with the potential to knockdown five isoforms of murine Cyp2b. This construct was used to generate the first persistent quintuple Cyp2b knockout mouse for the subsequent study of Cyp2b functions *in vivo*.

The expression of hepatic Cyp2b isoforms is significantly repressed in the Cyp2b-KD mice (Figs. 2 and 3). Western blots with liver microsomes demonstrate a near complete abolishment of Cyp2b proteins in the liver of untreated mice, and QRT-PCR indicates that all the hepatic Cyp2b isoforms are repressed in males and all but Cyp2b9 is significantly repressed in females (Fig. 2). Furthermore, TCPOBOP-mediated Cyp2b induction did not outcompete the shRNA's ability to repress Cyp2b protein expression, demonstrating that the Cyp2b-KD mouse model is functional in the presence of a CAR activator and powerful Cyp2b inducer (Fig. 3). Therefore, we have produced an efficient knockdown of at least the three major hepatic Cyp2b members in mice, including the highly inducible Cyp2b10.

In addition, parathion metabolism was significantly lower in hepatic microsomes from untreated and TCPOBOP-induced Cyp2b-KD mice than WT mice (Fig. 6). In a previous study, liver microsomes from CAR-null mice that have lower expression of several Cyps including Cyp2b and Cyp3a subfamily members compared with their WT counterparts, metabolize parathion slowly compared with WT mice. Furthermore, CAR-null mice show increased sensitivity to this organophosphate pesticide (Mota *et al*., 2010). Therefore, we examined the role of Cyp2bs in the metabolism of parathion in Cyp2b-KD mice. We observed that parathion metabolism is perturbed in the hepatic microsomes of untreated and TCPOBOP-induced Cyp2b-KD mice, and parathion toxicity is greater in Cyp2b-KD mice than WT mice (Fig. 7).

Previous studies with rats, chemically induced liver microsomes, and recombinant human CYPs also indicate a key role for Cyp2b in parathion metabolism, fate, and toxicity (Foxenberg *et al*., 2007, 2011; Kim *et al*., 2005; Mota *et al*., 2010; Mutch *et al*., 1999). Parathion toxicity is caused by its bioactivation to the toxic metabolite paraoxon (Sultatos *et al*.,

1984), but we observed reduced paraoxon production in the Cyp2b-KD mice that is not consistent with decreased toxicity. Similar but stronger results were obtained with the CAR-null mice (Mota *et al*., 2010). This suggests that toxicity in the Cyp2b-KD mice is due to poor metabolism of parathion to PNP (lower PNP/POXON ratio), which is also catalyzed by Cyp2b (Foxenberg *et al*., 2007, 2011; Mutch and Williams, 2006), extrahepatic metabolism of parathion, or higher clearance of paraoxon from the liver of Cyp2b-KD mice compared with WT mice because of poor metabolism of parathion and paraoxon. Liver perfusion studies indicate that parathion metabolized to paraoxon may exit the liver as paraoxon and cause toxicity (Sultatos *et al*., 1985). Overall, this study demonstrates that *in vivo* Cyp2b isoforms play a key role in parathion metabolism and toxicity, and this is the first study to demonstrate that individuals with compromised Cyp2b are susceptible to the toxic effects of parathion and suggests that active phase I metabolism of parathion is important for further metabolic deactivation and elimination.

ZOX paralysis time is a key indicator of perturbations in Cyp activity *in vivo*. Female Cyp2b-KD mice did not recover from Zox injection indicating poor metabolism and clearance and indicating a key role of Cyp2b in Zox metabolism. In contrast, male Cyp2b-KD mice did not demonstrate a significant difference in Zox paralysis time (Table 2). Most Cyp2bs (Cyp2b9, Cyp2b13, and may be Cyp2b10) are female predominant (Hernandez *et al*., 2006, 2009a; Wiwi *et al*., 2004), and therefore, reducing Cyp2b levels in female mice may cause a more pronounced effect. FVB (WT) mice also metabolize Zox better than B6 mice, and a higher dose is needed to cause paralysis (Hernandez *et al*., 2006). A 450 mg/kg dose appeared to be too high in a previous study (Hernandez *et al*., 2006), and therefore, we performed a pilot study and based on those results decided to use 400 mg/kg. However, this dose did not significantly affect the FVB male mice as few of them (WT and Cyp2b-KD) were fully paralyzed by Zox.

Histopathology demonstrated that female Cyp2b-KD mice did not respond to TCPOBOP treatment as expected and in turn showed perturbed histopathology parameters. Overall, though, the Cyp2b-KD mice are viable, fertile, and did not exhibit obvious gross abnormalities with the exception of an increase in liver weight. Liver enlargement has been regarded as a marker of drug associated enzyme induction and suggests a compensatory mechanism (Amacher *et al*., 2001; Webber *et al*., 1994), probably to adapt to increased concentrations of an endobiotic. Similar increases in hepatosomatic indices have been observed in other transgenic mice with low Cyp activity, including mice that lack key hepatic transcription factors that regulate Cyps. Examples include the hepatic POR-null mouse model (Henderson *et al*., 2003) and HNF4α-null mice (Hayhurst *et al*., 2001) where the liver/body weight ratios probably increased because of the accumulation of lipids. However, similar effects have not been reported in the Cyp3a-null mouse (van Herwaarden *et al*., 2007).

Interestingly, there also appears to be a molecular compensatory reaction to the repression of Cyp2bs in the Cyp2b-KD mice. For example, Cyp2b9 mRNA expression was not repressed in female Cyp2b-KD mice. Furthermore, no TCPOBOP-treated male mice showed repression of Cyp2b mRNA transcript levels, and female mice actually demonstrated greater expression of Cyp2b10 and Cyp2b13 in Cyp2b-KD mice following TCPOBOP treatment than WT mice. This suggests that there is some type of compensatory mechanism trying to overcome the repressive effects of the shRNA. CAR basally regulates Cyp2b10 and Cyp2b13 and may in part regulate Cyp2b9 (Hernandez *et al*., 2009b; Mota *et al*., 2010). Therefore, we hypothesized that CAR may be induced in order to adapt to the lack of Cyp2b members, especially Cyp2b10, in the Cyp2b-KD mice. CAR protein levels are increased in TCPOBOP-treated females, and this may help the mice adapt to lower Cyp2b expression and in turn increase Cyp2b mRNA expression. In addition to CAR, forkhead box protein A2 (FoxA2 also known as hepatic nuclear factor 3β), a female predominant transcription factor, regulates Cyp2b9 (Hashita *et al*., 2008), and therefore, this transcription factor may also play a role in the lack of Cyp2b9 repression in untreated and TCPOBOP-treated Cyp2b-KD female mice. Other transcription factors that in part regulate the sexually dimorphic expression of Cyp2b9, such as HNF4α and Stat5b, cannot be ruled out (Wiwi *et al*., 2004). Lastly, the compensatory induction of Cyp2b10 in males and females may just be due to increased retention of TCPOBOP caused by the lack of Cyp2b proteins, leading to greater activation of CAR and in turn higher Cyp2b10 transcript levels.

Even though Cyp2b transcript levels were increased in Cyp2b-KD mice to levels equal to or greater than WT mice following TCPOBOP treatment, protein expression was still much lower in the Cyp2b-KD mice. It has been suggested that Western blots are more reliable to confirm the efficacy of siRNA (Holmes *et al*., 2010). There are several potential reasons for this including the extracted RNA is nuclear or not available for siRNA degradation, or the 3′mRNA cleavage products resulting from siRNA-mediated cleavage accumulate within the cell (Holen *et al*., 2002), but are still large enough fragments that they result in small templates for cDNA synthesis and give rise to a false signal of mRNA detection by QRT-PCR (Holmes *et al*., 2010).

The long-term stability of the Cyp2b-KD transgene is not known. Lentiviral-mediated transgenesis following perivitelline injection has been shown to be stable for a couple of generations (Park, 2007); however, there have been few studies that have examined multigenerational stability of shRNAs. There are several potential problems that can arise as a shRNA transgenic line is propagated, including selective pressures from integration into transcriptionally active genes, methylation of the promoter, or a reduction in insert copy number, and all of these may lead to reduced functional transgene expression (Kong *et al*., 2009; Sauvain *et al*., 2008). Dilution

of the number of insert sites will occur as mice are mated to WT mice (Sauvain *et al*., 2008), and this may diminish the phenotype in subsequent generations. Conversely, one of the major advantages of viral-mediated transgenesis is the ability to produce mice with multiple integrants and therefore greater shRNA expression. In addition, shRNA can knockdown multiple genes with one construct or produce a large number of mice in a short period of time without the necessity of breeding (Lois *et al*., 2002; Park, 2007). For example, all 134 mice produced from our initial injections were positive, providing a vast number of mice for experimentation in a short period of time.

The shRNA generated Cyp2b-KD mice demonstrate low expression of hepatic Cyp2b members in untreated and TCPOBOP-treated mice. They also poorly metabolize the Cyp2b substrates Zox and parathion and in turn are sensitive to these toxicants, indicating that Cyp2bs play a key role in protecting individuals from select chemicals. Therefore, Cyp2b-KD mice may be able to act as a sentinel for individuals with low Cyp2b expression or limited metabolic capacity because of Cyp2b polymorphisms. Furthermore, this model can be built upon to form even better models for human disease, human metabolism, and human genetic polymorphisms by making CYP2B6/7-humanized mice. This study provides a new platform for studying Cyp2b function and especially its role in the metabolism of distinct pharmaceuticals and environmental chemicals.

SUPPLEMENTARY DATA

Supplementary data are available online at http://toxsci.oxfordjournals.org/.

FUNDING

National Institutes of Health grant R15-ES017321; a South Carolina EPSCoR/IDEA CCD project; a grant from the Clemson University Research Foundation; and Clemson University start-up funds.

REFERENCES

Amacher, D. E., Schomaker, S. J., and Burkhardt, J. E. (2001). The relationship among microsomal enzyme induction, liver weight and histological change in beagle dog toxicology studies. *Food Chem. Toxicol.* **39,** 817–825.

Athirakul, K., Bradbury, J. A., Graves, J. P., DeGraff, L. M., Ma, J., Zhao, Y., Couse, J. F., Quigley, R., Harder, D. R., Zhao, X., *et al*. (2008). Increased blood pressure in mice lacking cytochrome P450 2j5. *FASEB J.* **22,** 4096–4108.

Baldwin, W. S., Marko, P. B., and Nelson, D. R. (2009). The cytochrome P450 (CYP) gene superfamily in Daphnia Pulex. *BMC Genomics* **10,** 169.

Banks, W. J. (1993). In *Applied Veterinary Histology*, 3rd ed. C V Mosby, St Louis, MO.

Beilke, L. D., Aleksunes, L. M., Holland, R. D., Besselsen, D. G., Beger, R. D., Klaassen, C. D., and Cherrington, N. J. (2009). Constitutive androstane receptor-mediated changes in bile acid composition contributes to hepatoprotection from lithocholic acid-induced liver injury in mice. *Drug Metab. Dispos.* **37,** 1035–1045.

Blanco-Bose, W. E., Murphy, M. J., Ehninger, A., Offner, S., Dubey, C., Huang, W., Moore, D. D., and Trumpp, A. (2008). C-myc and its target foxm1 are critical downstream effectors of constitutive androstane receptor (CAR) mediated direct liver hyperplasia. *Hepatology* **48,** 1302–1311.

Blesch, A. (2004). Lentiviral and MLV based retroviral vectors for ex vivo and in vivo gene transfer. *Methods* **33,** 164–172.

Burns, J. C., Friedmann, T., Driever, W., Burrascano, M., and Yee, J. K. (1993). Vesicular stomatitis virus G glycoprotein pseudotyped retroviral vectors: Concentration to very high titer and efficient gene transfer into mammalian and nonmammalian cells. *Proc. Natl. Acad. Sci. U.S.A.* **90,** 8033–8037.

Ekins, S., Vandenbranden, M., Ring, B. J., Gillespie, J. S., Yang, T. J., Gelboin, H. V., and Wrighton, S. A. (1998). Further characterization of the expression in liver and catalytic activity of CYP2B6. *J. Pharmacol. Exp. Ther.* **286,** 1253–1259.

Elbashir, S. M., Lendeckel, W., and Tuschl, T. (2001). RNA interference is mediated by 21- and 22-nucleotide RNAs. *Genes Dev.* **15,** 188–200.

Finger, J. H., Smith, C. M., Hayamizu, T. F., McCright, I. J., Eppig, J. T., Kadin, J. A., Richardson, J. E., and Ringwald, M. (2011). The mouse Gene Expression Database (GXD): 2011 update. *Nucleic Acids Res.* **39**(Suppl. 1), D835–D841.

Foxenberg, R. J., Ellison, C. A., Knaak, J. B., Ma, C., and Olson, J. R. (2011). Cytochrome P450-specific human PBPK/PD models for the organophosphorus pesticides: Chlorpyrifos and parathion. *Toxicology* **285,** 57–66.

Foxenberg, R. J., McGarrigle, B. P., Knaak, J. B., Kostyniak, P. J., and Olson, J. R. (2007). Human hepatic cytochrome P450-specific metabolism of parathion and chlorpyrifos. *Drug Metab. Dispos.* **35,** 189–193.

Hashita, T., Sakuma, T., Akada, M., Nakajima, A., Yamahara, H., Ito, S., Takesako, H., and Nemoto, N. (2008). Forkhead box A2-mediated regulation of female-predominant expression of the mouse cyp2b9 gene. *Drug Metab. Dispos.* **36,** 1080–1087.

Hayhurst, G. P., Lee, Y. H., Lambert, G., Ward, J. M., and Gonzalez, F. J. (2001). Hepatocyte nuclear factor 4alpha (nuclear receptor 2a1) is essential for maintenance of hepatic gene expression and lipid homeostasis. *Mol. Cell. Biol.* **21,** 1393–1403.

Henderson, C. J., Otto, D. M., Carrie, D., Magnuson, M. A., McLaren, A. W., Rosewell, I., and Wolf, C. R. (2003). Inactivation of the hepatic cytochrome P450 system by conditional deletion of hepatic cytochrome P450 reductase. *J. Biol. Chem.* **278,** 13480–13486.

Hernandez, J. P., Chapman, L. M., Kretschmer, X. C., and Baldwin, W. S. (2006). Gender specific induction of cytochrome P450s in nonylphenol-treated FVB/NJ mice. *Toxicol. Appl. Pharmacol.* **216,** 186–196.

Hernandez, J. P., Huang, W., Chapman, L. M., Chua, S., Moore, D. D., and Baldwin, W. S. (2007). The environmental estrogen, nonylphenol, activates the constitutive androstane receptor (CAR). *Toxicol. Sci.* **98,** 416–426.

Hernandez, J. P., Mota, L. C., and Baldwin, W. S. (2009a). Activation of CAR and PXR by dietary, environmental and occupational chemicals alters drug metabolism, intermediary metabolism, and cell proliferation. *Curr. Pharmacogenomics Person. Med.* **7,** 81–105.

Hernandez, J. P., Mota, L. C., Huang, W., Moore, D. D., and Baldwin, W. S. (2009b). Sexually dimorphic regulation and induction of P450s by the constitutive androstane receptor (CAR). *Toxicology* **256,** 53–64.

Hodgson, E., and Rose, R. L. (2007). The importance of cytochrome P450 2B6 in the human metabolism of environmental chemicals. *Pharmacol. Ther.* **113,** 420–428.

Holen, T., Amarzguioui, M., Wiiger, M. T., Babaie, E., and Prydz, H. (2002). Positional effects of short interfering RNAs targeting the human coagulation trigger tissue factor. *Nucleic Acids Res.* **30,** 1757–1766.

Holmes, K., Williams, C. M., Chapman, E. A., and Cross, M. J. (2010). Detection of siRNA induced mRNA silencing by RT-qPCR: Considerations for experimental design. *BMC Res. Notes* **3,** 53.

Honkakoski, P., Zelko, I., Sueyoshi, T., and Negishi, M. (1998). The nuclear orphan-receptor CAR-retinoid X receptor heterodimer activates the phenobarbital-responsive module of the CYP2B gene. *Mol. Cell. Biol.* **18,** 5652–5658.

Jarukamjorn, K., Sakuma, T., Jaruchotikamol, A., Ishino, Y., Oguro, M., and Nemoto, N. (2006). Modified expression of cytochrome P450 mRNAs by growth hormone in mouse liver. *Toxicology* **219,** 97–105.

Jarukamjorn, K., Sakuma, T., Miyaura, J. I., and Nemoto, N. (1999). Different regulation of the expression of mouse hepatic cytochrome P450 2B enzymes by glucocorticoid and phenobarbital. *Arch. Biochem. Biophys.* **369,** 89–99.

Kim, D. O., Lee, S. K., Jeon, T. W., Jin, C. H., Hyun, S. H., Kim, E. J., Moon, G. I., Kim, J. A., Lee, E. S., Lee, B. M., *et al.* (2005). Role of metabolism in parathion-induced hepatotoxicity and immunotoxicity. *J. Toxicol. Environ. Health A* **68,** 2187–2205.

Kong, Q., Wu, M., Huan, Y., Zhang, L., Liu, H., Bou, G., Luo, Y., Mu, Y., and Liu, Z. (2009). Transgene expression is associated with copy number and cytomegalovirus promoter methylation in transgenic pigs. *PLoS One* **4,** e6679. doi:10.1371/journal.pone.0006679.

Kretschmer, X. C., and Baldwin, W. S. (2005). CAR and PXR: Xenosensors of endocrine disrupters? *Chem. Biol. Interact.* **155,** 111–128.

Lamba, V., Lamba, J., Yasuda, K., Strom, S., Davila, J., Hancock, M. L., Fackenthal, J. D., Rogan, P. K., Ring, B., Wrighton, S. A., *et al.* (2003). Hepatic CYP2B6 expression: Gender and ethnic differences and relationship to CYP2B6 genotype and CAR (constitutive androstane receptor) expression. *J. Pharmacol. Exp. Ther.* **307,** 906–922.

Lang, T., Klein, K., Richter, T., Zibat, A., Kerb, R., Eichelbaum, M., Schwab, M., and Zanger, U. M. (2004). Multiple novel nonsynonymous cyp2b6 gene polymorphisms in Caucasians: Demonstration of phenotypic null alleles. *J. Pharmacol. Exp. Ther.* **311,** 34–43.

Lee, J. S., Ward, W. O., Liu, J., Ren, H., Vallanat, B., Delker, D., and Corton, J. C. (2011). Hepatic xenobiotic metabolizing enzyme and transporter gene expression through the life stages of the mouse. *PLoS One* **6,** e24381.

Lee, S. S. T., Buters, J. T. M., Pineau, T., Fernandez-Salguero, P., and Gonzalez, F. J. (1996). Role of CYP2E1 in the hepatotoxicity of acetaminophen. *J. Biol. Chem.* **271,** 12063–12067.

Lois, C., Hong, E. J., Pease, S., Brown, E. J., and Baltimore, D. (2002). Germline transmission and tissue-specific expression of transgenes delivered by lentiviral vectors. *Science* **295,** 868–872.

Mateeva, O., Nechipurenko, Y., Rossil, L., Moore, B., Saetrom, P., Aleksey, Y., Ogurtsov, Y., Atkins, J. F., and Shabalina, S. A. (2007). Comparison of approaches for rational siRNA design leading to a new efficient and transparent method. *Nucleic Acids Res.* **35,** e63.

Mota, L. C., Hernandez, J. P., and Baldwin, W. S. (2010). CAR-null mice are sensitive to the toxic effects of parathion: Association with reduced CYP-mediated parathion metabolism. *Drug Metab. Dispos.* **38,** 1582–1588.

Mota, L. C., Hernandez, J. P., Barfield, C., and Baldwin, W. S. (2011). Nonylphenol-mediated CYP induction is PXR-dependent: The use of humanized mice and human hepatocytes suggests that hPXR is less sensitive than mouse PXR to nonylphenol treatment. *Toxicol. Appl. Pharmacol.* **252,** 259–267.

Muerhoff, A. S., Griffin, K. J., and Johnson, E. F. (1994). The peroxisome proliferator-activated receptor mediates the induction of CYP4A6, a cytochrome P450 fatty acid omega-hydroxylase, by clofibric acid. *J. Biol. Chem.* **267,** 19051–19053.

Muller, P. Y., Janovjak, H., Miserez, A. R., and Dobbie, Z. (2002). Processing of gene expression data generated by quantitative real-time RT-PCR. *Biotechniques* **32,** 1372–1379.

Mutch, E., Blain, P. G., and Williams, F. M. (1999). The role of metabolism in determining susceptibility to parathion toxicity in man. *Toxicol. Lett.* **107,** 177–187.

Mutch, E., and Williams, F. M. (2006). Diazinon, chlorpyrifos and parathion are metabolised by multiple cytochrome P450 in human liver. *Toxicology* **224,** 22–32.

Nelson, D. R., Zeldin, D. C., Hoffman, S. M. G., Maltais, L. J., Wain, H. M., and Nebert, D. W. (2004). Comparison of cytochrome P450 (CYP) genes from the mouse and human genomes, including nomenclature recommendations for genes, pseudogenes and alternative splice variants. *Pharmacogenetics* **14,** 1–18.

Park, F. (2007). Lentiviral vectors: Are they the future of animal transgenesis? *Physiol. Genomics* **31,** 159–173.

Percy, D. H., and Barthold, S. W. (2001). *Pathology of Laboratory Rodents and Rabbits.* Iowa State University Press, Ames, IA.

Ramezani, A., and Hawley, R. G. (2002). Generation of HIV-1-based lentiviral vector particles. *Curr. Protoc. Mol. Biol.* Chapter 16, Unit 16.22.

Reschly, E. J., and Krasowski, M. D. (2006). Evolution and function of the NR1I nuclear hormone receptor subfamily (VDR, PXR, and CAR) with respect to metabolism of xenobiotics and endogenous compounds. *Curr. Drug Metab.* **7,** 349–365.

Sastry, L., Johnson, T., Hobson, M. J., Smucker, B., and Cornetta, K. (2002). Titering lentiviral vectors: Comparison of DNA, RNA and marker expression methods. *Gene Ther.* **9,** 1155–1162.

Sauvain, M. O., Dorr, A. P., Stevenson, B., Quazzola, A., Naef, F., Wiznerowicz, M., Schütz, F., Jongeneel, V., Duboule, D., Spitz, F., *et al.* (2008). Genotypic features of lentivirus transgenic mice. *J. Virol.* **82,** 7111–7119.

Sultatos, L. G., Minor, L. D., and Murphy, S. D. (1985). Metabolic activation of phosphorothioate pesticides: Role of the liver. *J. Pharmacol. Exp. Ther.* **232,** 624–628.

Sultatos, L. G., Shao, M., and Murphy, S. D. (1984). The role of hepatic biotransformation in mediating the acute toxicity of the phosphorothionate insecticide chlorpyrifos. *Toxicol. Appl. Pharmacol.* **73,** 60–68.

Sutton, C. W., Sutherland, M., Shnyder, S., and Patterson, L. H. (2010). Improved preparation and detection of cytochrome P450 isoforms using MS methods. *Proteomics* **10,** 327–331.

Tang, J., Cao, Y., Rose, R. L., Brimfield, A. A., Dai, D., Goldstein, J. A., and Hodgson, E. (2001). Metabolism of chlorpyrifos by human cytochrome P450 isoforms and human, mouse and rat liver microsomes. *Drug Metab. Dispos.* **29,** 1201–1204.

Tzameli, I., Pissios, P., Schuetz, E. G., and Moore, D. D. (2000). The xenobiotic compound 1,4-bis[2-(3,5-dichloropyridyloxy)]benzene is an agonist ligand for the nuclear receptor CAR. *Mol. Cell. Biol.* **20,** 2951–2958.

Uppal, H., Toma, D., Saini, S. P., Ren, S., Jones, T. J., and Xie, W. (2005). Combined loss of orphan receptors PXR and CAR heightens sensitivity to toxic bile acids in mice. *Hepatology* **41,** 168–176.

Van der Hoeven, T. A., and Coon, M. J. (1974). Preparation and properties of partially purified cytochrome P450 and NADPH-cytochrome P450 reductase from rabbit liver microsomes. *J. Biol. Chem.* **249,** 6302–6310.

van Herwaarden, A. E., Wagenaar, E., van der Kruijssen, C. M. M., van Waterschoot, R. A. B., Smit, J. W., Song, J. Y., van der Valk, M. A., van Tellingen, O., van der Hoorn, J. W. A., Rosing, H., *et al.* (2007). Knockout of cytochrome P450 3A yields new mouse models for understanding xenobiotic metabolism. *J. Clin. Invest.* **117,** 3583–3592.

Wang, H., Faucette, S., Sueyoshi, T., Moore, R., Ferguson, S., Negishi, M., and LeCluyse, E. L. (2003). A novel distal enhancer module regulated by pregnane X receptor/constitutive androstane receptor is essential for the

maximal induction of CYP2B6 gene expression. *J. Biol. Chem.* **278,** 14146–14152.

Wang, H., and Tompkins, L. M. (2008). CYP2B6: New insights into a historically overlooked cytochrome P450 isozyme. *Curr. Drug Metab.* **9,** 598–610.

Waxman, D. J. (1988). Interactions of hepatic cytochromes P-450 with steroid hormones: Regioselectivity and stereoselectivity of steroid metabolism and hormonal regulation of rat P-450 enzyme expression. *Biochem. Pharmacol.* **37,** 71–84.

Waxman, D. J., Pampori, N. A., Ram, P. A., Agrawal, A. K., and Shapiro, B. H. (1991). Interpulse interval in circulating growth hormone patterns regulates sexually dimorphic expression of hepatic cytochrome p450. *Proc. Natl. Acad. Sci. U.S.A.* **88,** 6868–6872.

Webber, E. M., Wu, J. C., Wang, L., Merlino, G., and Fausto, N. (1994). Overexpression of transforming growth factor-alpha causes liver enlargement and increased hepatocyte proliferation in transgenic mice. *Am. J. Pathol.* **145,** 398–408.

Wei, P., Zhang, J., Egan-Hafley, M., Liang, S., and Moore, D. D. (2000). The nuclear receptor car mediates specific xenobiotic induction of drug metabolism. *Nature* **407,** 920–923.

Willingham, A. T., and Keil, T. (2004). A tissue specific cytochrome P450 required for the structure and function of *Drosophila* sensory organs. *Mech. Dev.* **121,** 1289–1297.

Wiwi, C. A., Gupte, M., and Waxman, D. J. (2004). Sexually dimorphic P450 gene expression in liver-specific hepatocyte nuclear factor 4α-deficient mice. *Mol. Endocrinol.* **18,** 1975–1987.

Yamada, H., Ishii, Y., Yamamoto, M., and Oguri, K. (2006). Induction of the hepatic cytochrome P450 2B subfamily by xenobiotics: Research history, evolutionary aspect, relation to tumorigenesis, and mechanism. *Curr. Drug Metab.* **7,** 397–409.

Zhang, J., Huang, W., Chua, S. S., Wei, P., and Moore, D. D. (2002). Modulation of acetaminophen-induced hepatotoxicity by the xenobiotic receptor CAR. *Science* **298,** 422–424.